Deriving wetland-cover types (WCTs) from integration of multispectral indices based on Earth observation data

Manudeo Singh · Satyasri Allaka · Praveen K. Gupta · J. G. Patel · Rajiv Sinha

Abstract The wetland cover is defined as the spatially homogenous region of a wetland attributed to the underlying biophysical conditions such as vegetation, turbidity, hydric soil, and the amount of water. Here, we present a novel method to derive the wetland-cover types (WCTs) combining three commonly used multispectral indices, NDVI, MNDWI, and NDTI, in three large Ramsar wetlands located in different geomorphic and climatic settings across India. These wetlands include the Kaabar Tal, a floodplain wetland in east Ganga Plains, Chilika Lagoon, a coastal wetland in eastern India, and Nal Sarovar in semi-arid western India. The novelty of our approach is that the derived WCTs are stable in space and time, and therefore, a given WCT across different wetlands or within different zones of a large wetland will imply similar underlying biophysical attributes. The WCTs can therefore provide a novel tool for monitoring and change detection of wetland cover types. We have automated the proposed WCT algorithm using the Google Earth Engine (GEE) environment and by developing ArcGIS tools. The method can be implemented on any wetland and using any multispectral imagery dataset with visible and NIR bands. The proposed methodology is simple yet robust and easy to implement and, therefore, holds significant importance in wetland monitoring and management.

Keywords Wetland dynamics · Wetland hydrology · Wetland management · Wetland monitoring · Wetland remote sensing

M. Singh · S. Allaka · R. Sinha (✉)
Department of Earth Sciences, Indian Institute of Technology Kanpur, Kanpur, India
e-mail: rsinha@iitk.ac.in

M. Singh
Institute of Geosciences, University of Potsdam, Potsdam, Germany

P. K. Gupta · J. G. Patel
Space Applications Centre, ISRO, Ahmedabad, India

Introduction

Earth's surface is a mosaic of various land cover types including numerous terrestrial and aquatic ecosystems. Driven by phenology and various biotic-abiotic processes, interactions, and disturbances, such ecosystems keep changing and are never a truly static system (Dronova et al., 2015; Oestreich et al., 2020). Land use/land cover (LULC) mapping and change detection amongst LULC classes is a way to understand the dynamic nature of such ecosystems. Generally, most LULC datasets focus on terrestrial systems and classify aquatic systems into broader categories such as waterbody, lakes, and wetlands (Dronova

et al., 2011, 2015; Singh & Sinha, 2021a). However, aquatic ecosystems such as wetlands undergo significant and frequent surface dynamics and are a mosaic of various cover types (Dronova et al., 2011, 2015; Singh & Sinha, 2021a). They are being subjected to long- and medium-term changes induced by climate change and land use (Taddeo & Dronova, 2018) as well as inter-seasonal changes in their vegetation and water spread areas induced by modifications in the hydrological cycle (Dronova et al., 2015; Hess et al., 2003; Singh & Sinha, 2021a, 2022; Singh et al., 2022). Therefore, such aquatic ecosystems require different approaches than generalised LULC classification schemes to understand their long-term behaviour and characteristic regimes (Dronova et al., 2015; Hess et al., 2003; Singh & Sinha, 2021a, b).

For aquatic ecosystems such as inland lakes and coastal waters, which may contain open water areas as the dominant cover type, the concept of optical water type (OWT) has been used by previous workers. The OWTs are based on various bio-optical models and classify the water based on the optical properties of water constituents such as chlorophyll, dissolved organic matter, and suspended matter (Moore et al., 2014). Another scheme, the Forel-Ule (FU) colour index, which is a visual colour comparison scale of water bodies ranging from blue to cola brown (type 1 to type 21) (Forel, 1890; Ule, 1892; Ye & Sun, 2022), has also been utilised to classify the water types. However, wetlands are a complex and heterogeneous mixture of various cover types ranging from vegetation (submerged, emerged, floaters), saturated soil, vegetated soil, varying water depths, and various water constituents. Therefore, the OWT and FU colour scale methods are not appropriate for characterising the wetland surface dynamics.

The concept of wetland cover types (WCT) was introduced in the early 1980s to understand the wetland dynamics and to identify the spectral characteristics of wetland habitat (Ernst-Dottavio et al., 1981). Most commonly, Landsat MSS and TM sensors have been used for wetland cover mapping in different parts of the world (Dottavio & Dottavio, 1984). For example, the Palo Verde National Park wetlands, Costa Rica have been studied to understand the impact of cattail (a wetland emergent vegetation) management activities (Trama et al., 2009) and evaporation rates of different cover types (Jiménez-Rodríguez et al., 2019). Mozumder et al. (2014) worked on the Deepor Beel

in India, a Ramsar site, to understand wetland dynamics. Dronova et al. (2015) mapped annual change cycles in the Poyang lake-wetland complex of China, and Fang et al. (2016) provided an assessment of the temporal dynamics of the Nanjishan wetland of China.

Both human activities and the natural environment control the changes in wetland cover types (Zhang et al., 2021). It is also well-established that the variability of aquatic diversity is a function of seasonally controlled water availability (Davidson et al., 2012). Therefore, water availability is the prime variable dictating a wetland's biotic and abiotic conditions and ecological services (Steinbach et al., 2021), rightly necessitating the inclusion of water variability in any wetland dynamics study. However, wetlands consist of various non-water cover types as well, which also control wetland hydrology by influencing the evaporation (Gehrels & Mulamoottil, 1990; Todd et al., 2006), especially in non-wet seasons (Jiménez-Rodríguez et al., 2019). Other variables, such as water temperature, are also affected by vegetation cover (Jiménez-Rodríguez et al., 2019). Further, soil, vegetation, and hydrology characterise the wetland's structure (Zhang et al., 2021).

A review of the current approaches of mapping WCT suggests that most of these are based on field identification of major cover patches in a wetland (Jiménez-Rodríguez et al., 2019) or satellite-imagery-based mapping using on-screen digitisation (Trama et al., 2009), object-oriented classification (e.g., Dronova et al., 2015; Zhang et al., 2021), or rule-based thresholding of multispectral indices (e.g., Mozumder et al., 2014). Also, these approaches are mostly tailored for specific wetlands and need customisation and readjustment to apply them to other wetlands. Further, these methods define cover types as 'static' units in terms of broad categories of cover patches and do not account for transitional or new cover types. Further, given the dynamic nature of wetlands and the need for long-term assessment, multi-temporal mapping is necessary. This necessitates a method wherein cover types (a) can attain dynamic values whenever needed, (b) should be invariant to spatio-temporal changes, and (c) can be automated with minimal human inputs.

The availability of medium spatial resolution satellite datasets such as Landsat series (30 m spatial resolution, 16 days repeatability) and Sentinel-2 series (10 m, 20 m, and 60 m spatial resolutions, 5–10 days

repeatability), augmented by cloud-computing facilities such as Google Earth Engine (GEE), long-term assessment and WCT generation for management and monitoring of wetlands is easier than ever. Here, we have developed a protocol to classify the dynamic WCTs based on the thresholding of multispectral indices. Our approach is novel in the sense that the derived WCTs are stable in space and time, and therefore, a given WCT across different wetlands or within different zones of a large wetland will imply similar underlying biophysical attributes. We have implemented the protocol in GEE scripts and have also designed a tool in ArcGIS to classify the WCTs for a given wetland automatically. We have applied this protocol to three different wetlands of India situated in different climatic and geographic locations and have discussed its utility for the management and monitoring wetlands. The WCTs have therefore the potential to become a novel tool for monitoring and change detection of wetland cover types.

Study areas

Kaabar Tal—a floodplain wetland

The Kaabar Tal (86°05′E—86°09′E and 25°30′N—25°32′N) is one of the largest freshwater wetlands in the Kosi-Ganga River interfluve in the North Bihar, eastern India (Singh & Sinha, 2020) (Fig. 1). The Kaabar Tal is primarily fed by the precipitation induced overland flow with a catchment area of approximately 195.6 km². The wetland experiences the monsoon season from July to September, with an average annual precipitation of 1200 mm. The maximum and minimum temperature of the wetland region varies from 25 to 38 °C in summer and 8 to 25 °C in winter, respectively. The Kaabar Tal was declared a protected area and a bird sanctuary in 1989, recognised later as a wetland of national importance by the Government of India, and was finally included in the list of Ramsar sites in 2021. This wetland is an important habitat for migratory and residential waterfowls belonging to 186 species and 41 families, including some threatened species such as the Sarus crane (*Grus antigone*), the white-rumped vulture (*Gyps bengalensis*), the greater spotted eagle (*Aquila clanga*), and the Indian vulture (*Gyps indicus*) (Ambastha et al., 2007).

Located in a tropical region, the Kaabar Tal is an excellent source for fishing, fodder, and agriculture, and has been overexploited in the recent years leading to its degradation. The Kaabar Tal wet area has been shrinking for the past 2 decades (1984–2020) (Singh & Sinha, 2021a, b), and the groundwater level is depleted drastically in the surrounding region (Sinha et al., 2018).

Chilika—a coastal lagoon

The Chilika (19°28′N—19°54′N and 85°05′E—85°38′E) is one of the largest brackish water lagoons in India with a catchment area of 3560 km² located in a tropical climate region on the eastern coast (Fig. 1). The Chilika was recognised as a wetland of international importance under the Ramsar Convention in 1981 and was designated a UNESCO world heritage site in 2019. The Chilika is one of the important biodiversity hotspots globally and attracts millions of migratory birds every year. More than 0.2 million people are completely dependent on the fish resources of the Chilika wetland.

The lagoon is fed by 52 rivers and rivulets that act as the source of the freshwater inflow from the north. The lagoon is connected to the seashore to the east by a 32 km long inlet channel that feeds saline water. With an average annual precipitation of 1238.8 mm, the wetland experiences NE and SW monsoons in June–September and November–December, respectively. Three other seasons in this region are winter from December to February, followed by summer from March to May and pre-monsoon from October to November. The maximum and minimum temperature in this region is 39.9 °C and 14.0 °C in summer and winter, respectively. The water spread area of Chilika varies from 900 to 1165 km² during the summer and monsoon seasons, respectively.

The Chilika is an estuary system in which sedimentation and salinity play dominant roles to determine the ecosystem of the wetland. During the summer season, the water level is lowest and this increases the salinity in the wetland. During the monsoon season, freshwater from the northern and eastern catchments carries sediments and nutrients into the wetland. During 1981–1993, the Chilika suffered a significant loss of biodiversity due to excessive siltation, a decrease in freshwater inflow, and shrinkage in the wetland area. Consequently, it
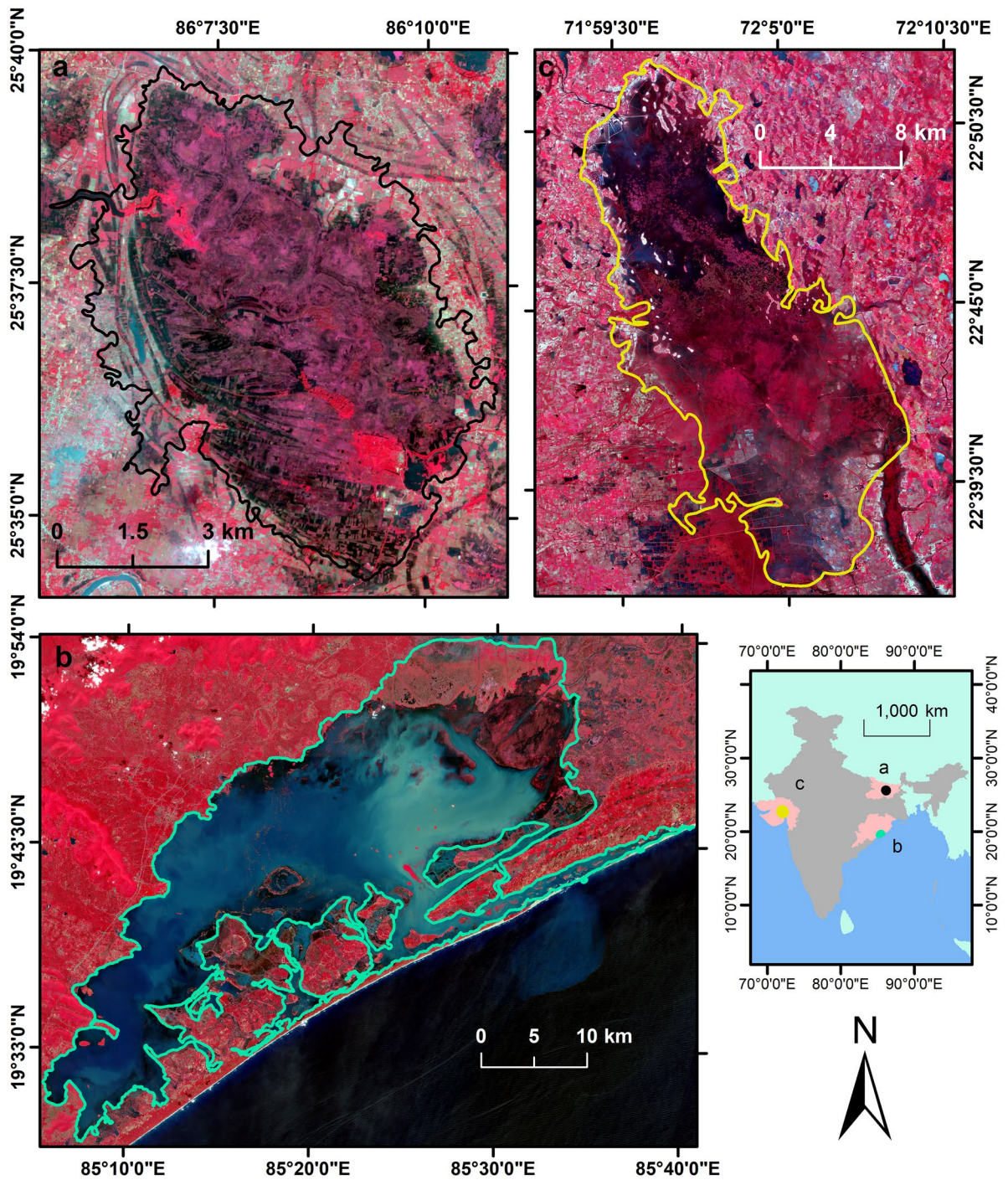
Fig. 1 Study areas **a** Kaabar Tal in Ganga Plains, **b** Chilika Lake—a coastal lagoon, and **c** Nal Sarovar, a semi-arid region lake

was added to the Montreux record of endangered wetlands in 1993 (Finlayson et al., 2020). However, it was removed from the Montreux record list in 2002 because of the exemplary remedial measures taken up by the Chilika Development Authority (CDA).

Nal Sarovar—a semi-arid region wetland

The Nal Sarovar (22°78′N—22°96′N and 71°78′E —72°64′E) is a bird sanctuary and a Ramsar wetland spread over 120 km^2 in semi-arid parts of Gujarat, western India (Fig. 1). The average monthly temperature ranges between 7 and 45 °C, and this region receives 700 mm of mean annual rainfall. The water spread area of this wetland is strongly a function of precipitation and can reach as high as 300 km^2 in an above-average monsoon year, 60 km^2 in an average rainfall year, 30 km^2 in a below-average rainfall year, to as low as 15 km^2 in a rainfall-scarce year (RIS, 2012). The Nal Sarovar is rich in aquatic avifauna— eighty-five bird species of 18 different families were recorded in this wetland in a multi-seasonal study between 2016 and 2018 by Joshi et al. (2020). Most of the bird species were recorded in the winter season (84 species) and the least in the summer season (50 species). The fluctuations in the water level of the wetland result in a highly dynamic avifauna habitat (Murthy & Panigrahy, 2011).

From the west, the Nal Sarovar is fed by two seasonal rivers—the Brahmini and Bhogavo and their tributaries. The flows from the surrounding areas also drain into the wetland during monsoons. Therefore, the hydrology of this wetland entirely depends on the monsoon rainfall, making the water spread area highly seasonal. The Nal Sarovar and its surrounding regions are rich in saline/alkaline salts, mostly concentrated in the upper layers of the soils (Tatu et al., 1999). This makes the water of this wetland brackish in post-monsoon and saline in springs and afterwards (Tatu et al., 1999). In most years, the wetland dries out by early summer (Chauhan, 2003).

Datasets and method

Wetlands are a mosaic of various cover types with unique biophysical properties such as open water, turbid water, several aquatic vegetations, and saturated soil. In dry seasons, wetlands also contain dry soil surfaces and terrestrial vegetation. All these cover types are optically sensitive in different regions of the electromagnetic spectrum and can be identified from satellite imageries using suitable indices. In this work, we first explored the specific indices which can distinguish wetland cover types. We initially selected

23 such indices (see Supplementary Information and Table S1), corresponding to different optically sensitive water constituents. We calculated these 23 indices for Chilika Lagoon using the Sentinel-2 dataset. Out of these 23 indices, we finally selected the three best suitable indices based on multivariate analysis such as principal component analysis (PCA), and detrended correspondence analysis (DCA), and visual analysis using ISO-clustering (see Supplementary Information and "Datasets and Method" section). Three selected indices (hereafter called WCT indices) are normalized difference water index (NDWI), normalized difference vegetation index (NDVI), and normalized difference turbidity index (NDTI), which correspond to water/wetness, vegetation, and turbidity/soil cover types of a wetland respectively. We selected NDWI instead of the more robust modified normalized difference water index (MNDWI) so that we could use 10 m spatial resolution bands (green and NIR) of Sentinel-2 instead of the SWIR bands with a coarse (20 m) spatial resolution. We intend to develop a wetland monitoring algorithm with widely available VNIR (visible and near-infrared) bands. The major steps of our algorithm are shown in Fig. 2.

In any pixel of satellite imagery of a wetland, all three constituents- water, vegetation, and turbidity, might be present. Such pixels are known as mixed pixels. The
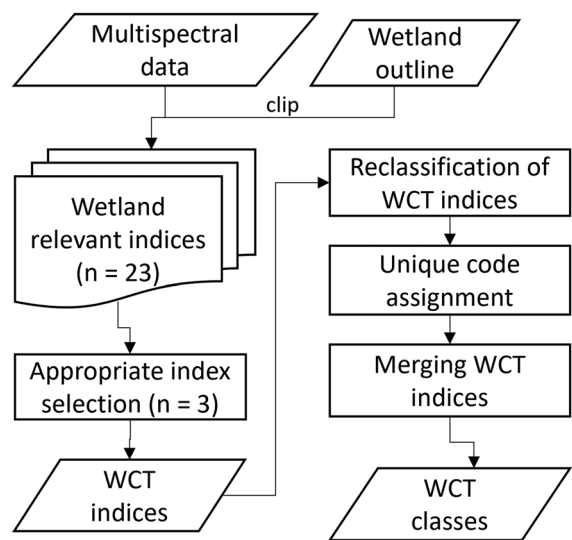

Fig. 2 Methodology for WCT demarcation. See Table S1 for indices list. NDWI, NDVI, NDTI are the WCT indices. See Table 1 for classes and codes of WCT indices

WCT indices account for the presence and relative proportion of such constituents in mixed pixels, and it is possible to assign a unique WCT class for each pixel. To preserve the information about the relative proportion of each constituent in the indices, we classified the positive values of the indices into four classes with equal intervals of 0.25 and assigned a unique key to each class (Table 1). Accordingly, if there is a pixel with low wetness (W1) and medium turbidity (T2), the WCT class for that pixel would be W1T2. If low vegetation cover is also present in the same pixel, the pixel would be classified as W1V1T2. Further, since all three indices range between (−) 1 and (+) 1; the positive values represent the presence of the constituent and a higher density of the constituent results into higher index values. For example, a pixel with an NDVI value of 0.8 (i.e., V4 class) will have a denser vegetation cover than a pixel with a value of 0.2 (i.e., V1 class).

Using four classes of indices instead of single threshold value to identify the cover types, we have provided an algorithm with the flexibility to produce dynamic WCTs. For example, if the vegetation cover in a pixel with medium wetness (W2) and low vegetation (V1), i.e., cover type W2V1, increases to V3 class, a new cover type W2V3 will result, reflecting the dynamic behaviour of that pixel. Furthermore, since the WCTs result from the underlying biophysical properties of wetlands and are estimated using indices, a given WCT class at some other time or some other place will represent similar underlying conditions. Therefore, the WCTs are invariant to spatiotemporal changes.

To understand the applicability of the WCT algorithm for the assessment of temporal dynamics of the wetlands, we chose three seasons—post-monsoon (October–November), spring (February), and pre-monsoon (May) and calculated the WCTs for 3 years namely, 2018–2019, 2019–2020, and 2020–2021. Further, we used Landsat-8 and Sentinel-2 surface reflectance datasets available in the GEE data repository and took median values of all available cloud-free datasets for each season. For wetland boundary delineation, we have used SRTM DEM (30 m) and Landsat series datasets and applied the DEM-based topographic index method (Sinha et al., 2017) and multispectral data-based time-series wetness-index method (Singh & Sinha, 2022) to extract the wetland boundaries in a GIS environment automatically. For Nal Sarovar and Chilika Lagoon, the boundaries were further cleaned using on-screen digitisation.

To evaluate the inter-sensor applicability of the WCT algorithm, we calculated the WCTs using Landsat-8 and Sentinel-2 datasets for all three wetlands. For Chilika and Nal Sarovar, we used Sentinel-2 imageries acquired on 1 Feb. 2021 and Landsat-8 imageries acquired on 2 Feb. 2021 and 1 Feb. 2021, respectively. For Kaabar Tal, we used Sentinel-2 imagery of 16 Feb. 2021 and Landsat-8 imagery of 18 Feb. 2021.

For validation of WCT classes, field data were collected on 3 and 4 Mar. 2020 from Kaabar Tal and on 7 and 8 Mar. 2020 from Chilika. The dates for field visits were selected to account for the Sentinel-2 acquisition date of 3 Mar. 2020 for both wetlands. The WCT classes were created for both wetlands using the Sentinel-2 imagery and then used for field validation. We also used the Parrot SEQUOIA multispectral camera to acquire in-situ data in VNIR bands red, green, near infrared and red edge at 1.2 MP and RGB image at 16 MP. The camera has an automatic radiometric calibration which provides the absolute reflectance measurements of the earth's surface features. The WCTs were also created from the imageries acquired from the multispectral camera and compared with the satellite-derived WCTs. Field locations were limited to major clusters due to logistic constraints and navigational issues across the wetlands.

We have implemented the WCT algorithm in Google Earth Engine (GEE) and have also developed ArcGIS tools to calculate the WCTs of any given wetland automatically. The GEE tool only requires the wetland polygon and desired time period as user inputs. The ArcGIS tool requires wetland polygon as shapefile and three multispectral bands green, red, and NIR in raster format. The GEE script and the ArcGIS tools are available on GitHub (https://github.com/manudeo/Wetland-Cover-Types) for public use. Since the scripts and tools are editable, the users can change the WCT indices as per the assessment goals.

Table 1 Defining unique keys for WCTs

Thresholds		Unique keys		
Range	Class	NDWI	NDVI	NDTI
0.0–0.25	Low	W1	V1	T1
0.25–0.50	Medium	W2	V2	T2
0.50–0.75	High	W3	V3	T3
0.75–1.0	Very high	W4	V4	T4

Further details about scripts and tools are provided in the Supplementary Information.

Results

Kaabar Tal

The WCTs of the Kaabar Tal for three seasons, namely, post-monsoon, spring, and pre-monsoon for 3 years, 2018–2019, 2019–2020, and 2020–2021 are shown in Fig. 3. Vegetation is the most dominant cover type in all seasons and for all years (WCT—V's), except for the pre-monsoon of 2019, when VT types are prevalent. Open-water types (W's) are generally negligible except for some patches in the post-monsoon period of 2019 and 2020 and the spring of 2020 and 2021. Field visits suggest that the central part of the wetland has water depths ranging from a few centimetres to 2 m. However, most of these regions are covered with dense aquatic vegetation, which is evident in WCTs. The VT types correspond
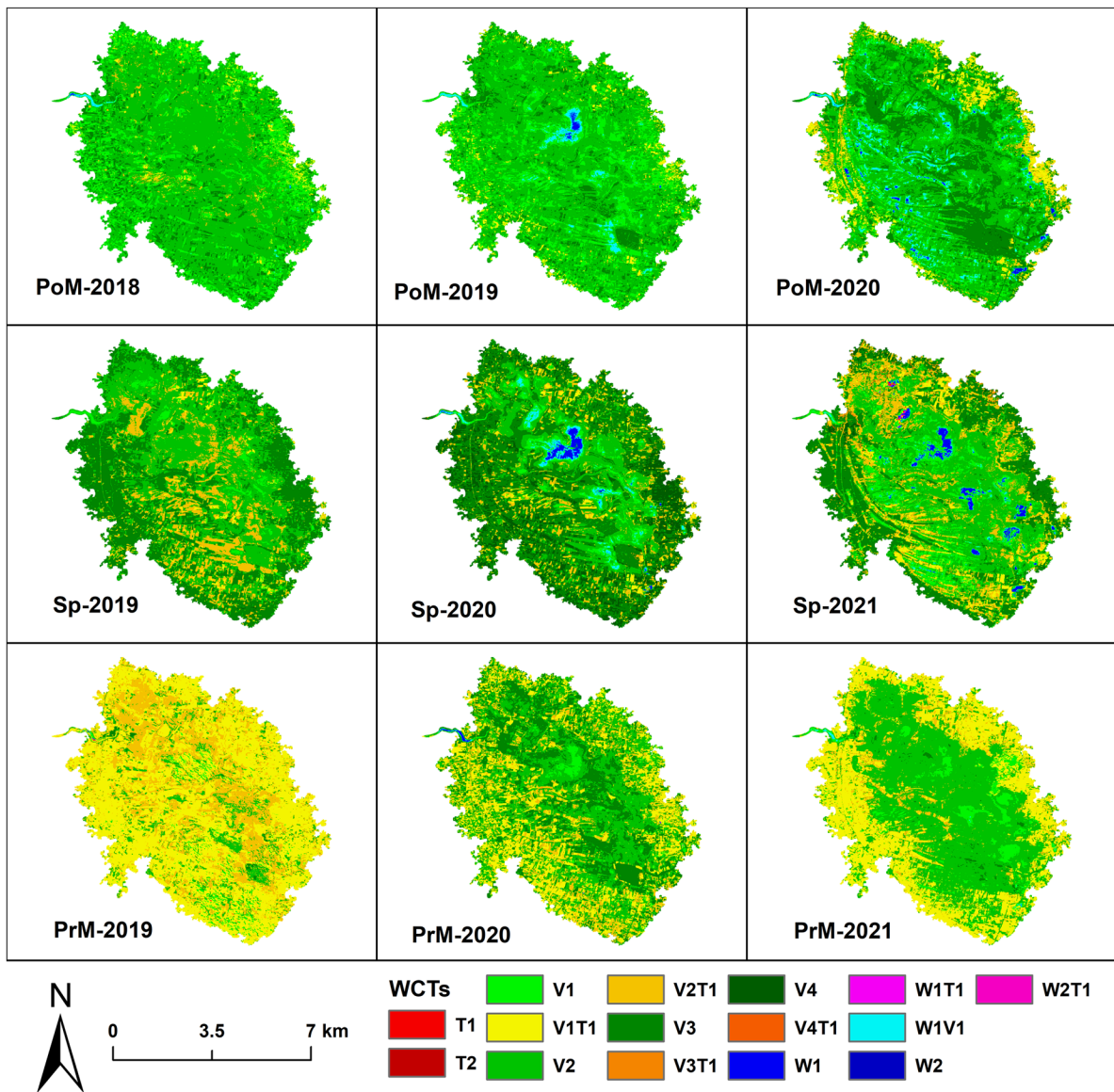
Fig. 3 Seasonal WCTs of Kaabar Tal for period 2018–2021. PoM: post-monsoon; Sp: spring; PrM: pre-monsoon

to vegetation with bare soil in dry areas and with turbid water in wet regions of the wetland. Along the margins of the wetland, the VT WCTs correspond to the regions which are now being used for agricultural purposes (e.g., pre-monsoon WCTs). The water spread area of this wetland is highly dynamic, and it is very common to find aquatic vegetation such as lotus in seemingly dry regions. Therefore, it is challenging to classify vegetation cover between aquatic and terrestrial based on WCTs only.

Apart from the water spread area dynamics, all WCTs also exhibit transformation from one type to another at a seasonal scale (Fig. 4). In Kaabar Tal, all seasons are dominated by vegetation-related WCTs. Between post-monsoon and spring, most of the V1 type (low vegetation) gets transformed into medium (V2/V2T1) or high (V3) vegetation cover types. Medium vegetation type (V2) occupies the largest area in all three seasons. Figure 4 provides a critical observation that even though the area of a

given cover type seems non-variant across seasons (e.g., V3 in post-monsoon and spring), the cover types are not fixed in space, and their location varies significantly across the wetland. For example, the total area covered by V3 in both post-monsoon and spring seasons is similar (~13 km^2), but only a fraction of V3 covered region of post-monsoon is stable in spring; the rest is attributed to the transformation from other WCTs such as V1, V2, V1T1, and V2T1. Therefore, it is critical to map these transformations rather than focusing on the change in the net area of a cover type for developing management strategies for such highly dynamic wetlands.

When the wetland system moves from a wet (post-monsoon) to a dry (pre-monsoon) regime, a reduction in vegetation cover is expected and can be observed by tracking dry region WCTs such as V1T1 and V2T1. The fully vegetated regions in post-monsoon (Vs) would normally transform into VT in spring and pre-monsoon. Contrary to this normal behaviour, the
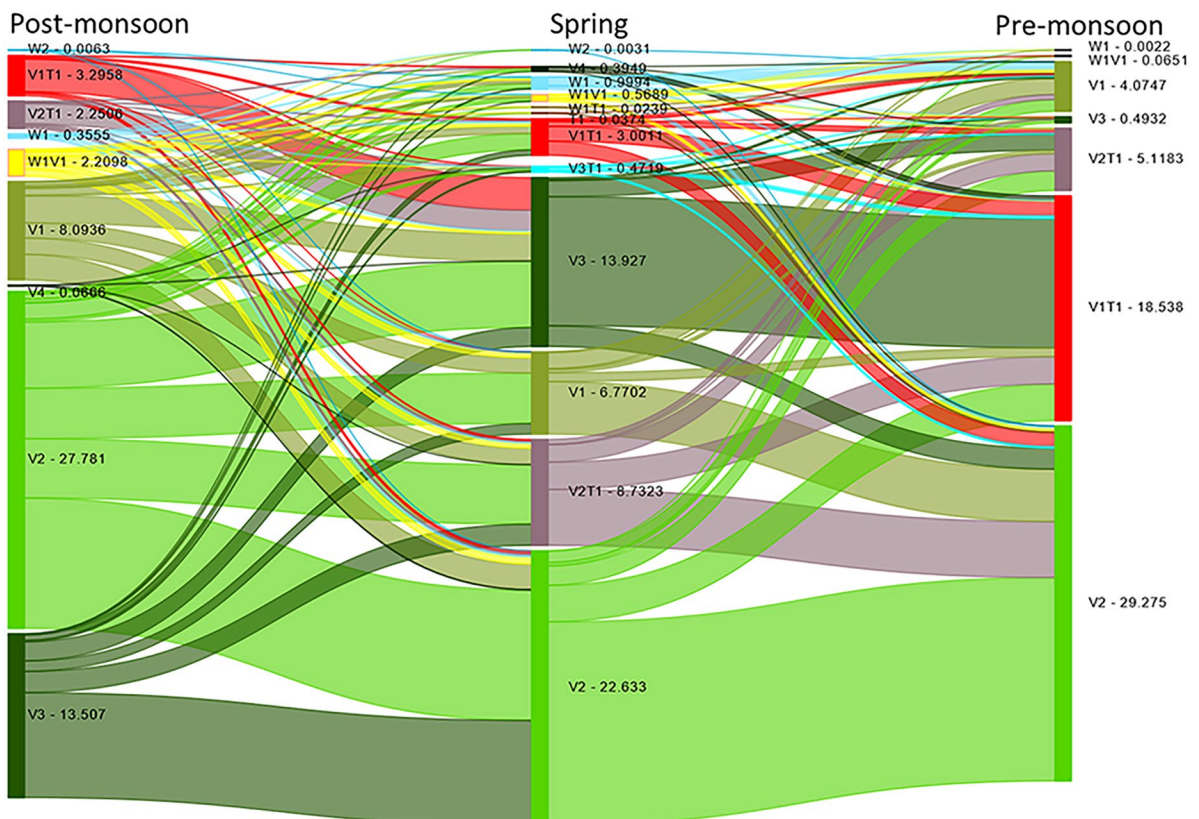

Fig. 4 Seasonal transformation of WCTs in Kaabar Tal in year 2020–2021. Numbers are representing areas of corresponding WCT in km^2

Kaabar shows a conversion of V1T1 of post-monsoon to V3 of spring, which is attributed to agricultural practices in the wetland area (see margins in post-monsoon 2020 and spring 2021 in Fig. 3).

Although the WCTs from the handheld camera (Parrot SEQUOIA) are of much higher resolution (10^{-3} m versus 10^1 m), in general, they are in agreement with the satellite-derived WCTs (Fig. 5). Open water is correctly characterised as W classes of WCTs in both imageries. However, in some areas, aquatic vegetation is classified as Vs in satellite imagery and not as WVs (Fig. 5(d)) and this reflects the sensors' limitation to capture water depth variations. Problems with high-resolution multispectral imageries from SEQUOIA are also evident where noise (e.g., shadows) is also classified as WCTs (as turbid WCT and WTs). However, a high-resolution sensor is also able to capture the variability of the wetland cover in greater detail, as evident by diverse WCTs classes in multispectral data from the handheld camera (Fig. 5(b2) and (c2)).

Chilika

The Chilika receives a continuous inflow of fresh water from its northern catchment and saline water through its mouth into the Bay of Bengal to the east. Therefore, this wetland has no issues with water availability, which is evident from the water-dominated WCTs in all seasons and for all years (Fig. 6). However, the freshwater inflow in the northern region also brings sediments with them, resulting in plumes of turbid water (WT types), mostly in the northern region. The same northern part also consists of highly dense emergent vegetation (reeds), captured here as V-type wetland covers. The central and north-western regions are also rich in submergent vegetation, but Sentinel-2 sensors could not map this. The northern region (inlets of fresh water) and the eastern linear region towards the sea display the most dynamic WCTs. In the northern part, the extent and intensity of vegetation (V types) in the post-monsoon season are increasing with time. Turbid water cover (W1T1) is also growing with time for the same season. Turbid WCTs are primarily absent in spring but reappear in pre-monsoon, with pre-monsoon of 2019 showing an extensive coverage of turbid WCT (Fig. 6). Barring the northern, eastern, and near-shore regions, other regions are not so dynamic in terms of WCTs except for W types. The

WCTs corresponding to dry regions covered with vegetation (VT) are mostly present in small islands and close to the shore of the wetland. Aquatic vegetation-related WCTs (WV) are spread in different regions in different seasons and do not exhibit a stable pattern, in contrast to the V types in the north region. This is because the V types are emergent vegetation, and WV types are floating vegetation covers.

Although open water is the primary cover type of this wetland, its depth varies at a seasonal scale, and so do the W cover types (Fig. 7). In the post-monsoon season of 2020, the high-water cover type (W3) is the most dominant WCT, and 15 km^2 of very high-water cover type (W4) is also present in this season. However, W4 is absent in the other two seasons. Further, W3 is significantly reduced in spring and disappears in pre-monsoon. Therefore, the monsoon is also controlling this wetland significantly, even though it has perennial water sources. The WV cover type occupies ~19 km^2 of the area in post-monsoon 2020, increasing to ~33 km^2 in spring 2021 and ~32 km^2 in pre-monsoon 2021. However, it should be noted that only a small fraction of the WV type of post-monsoon is retained in spring, and most of the WV type of spring is transformed from the W types of post-monsoon. A similar relationship is observed for WV type between spring and pre-monsoon. However, in the case of V2 and V3, most regions do not change with the season. The turbid cover type occupied a very high area of ~64 km^2 during the post-monsoon period of 2020, which was reduced to only 1 km^2 in spring 2021 but increased again to ~17 km^2 in pre-monsoon 2021.

The WCTs derived for the Chilika wetland were validated by field visits (Fig. 8). Like Kaabar Tal, the overall WCT pattern in this wetland generated from the imageries captured from a high-resolution handheld camera matches with the moderate resolution WCTs of Sentinel-2. For example, a large patch of submerged vegetation in very shallow water and floating algal growth were observed in the wetland (Fig. 8(b1)), which was classified as WCT of Vs and WVs in the satellite imagery (Fig. 8(a1)) as well as in the handheld multispectral imagery (Fig. 8(b2)). Open water-related WCTs dominate this wetland (Fig. 8(a)), which is also validated from field observations (e.g., Fig. 8(b)). In the northern region, a large patch of V-type WCTs was mapped in all years (Fig. 6) represented by emergent vegetation (Fig. 8(d1)). Also, these regions receive
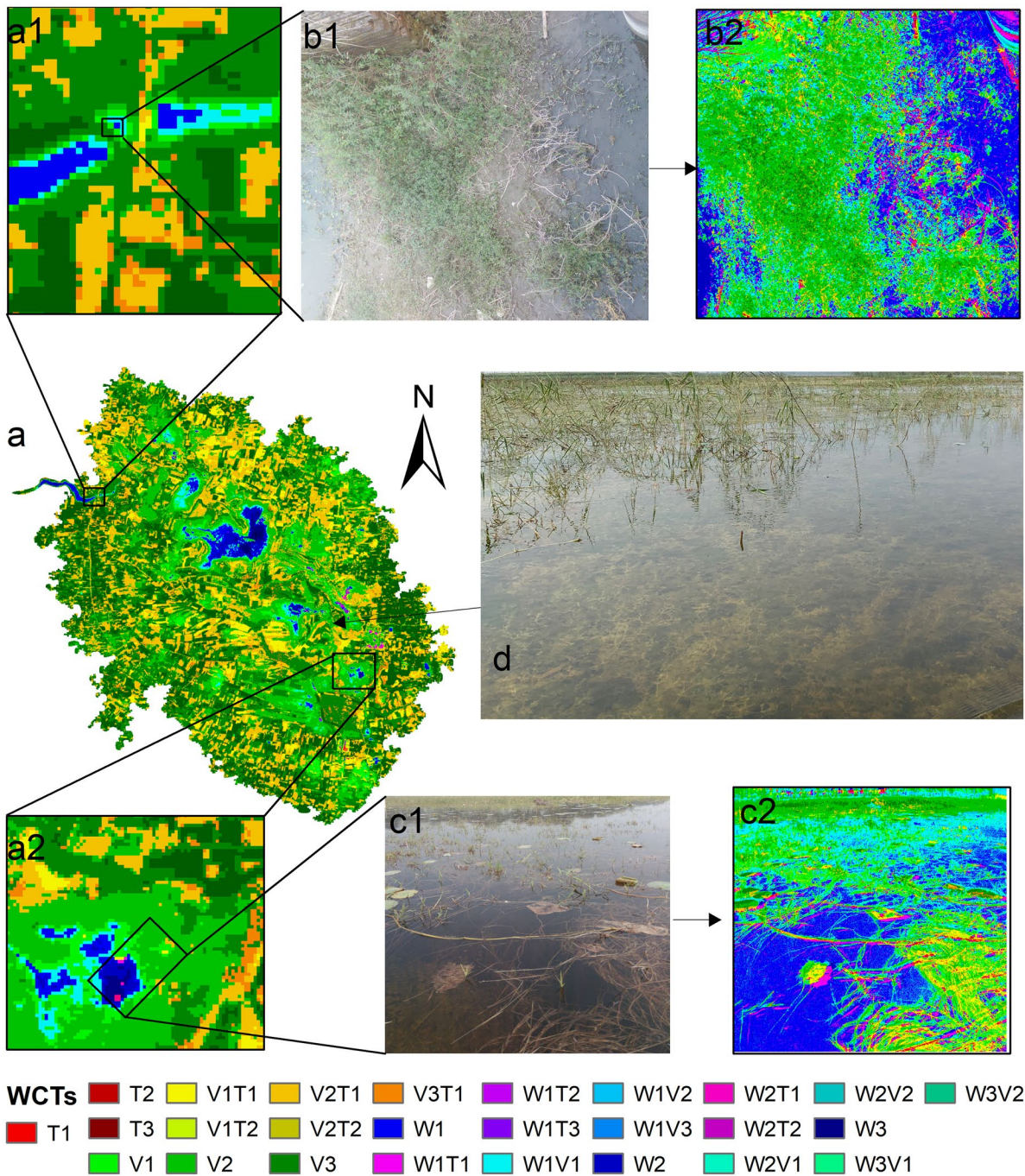
Fig. 5 Field validation—WCT classes of Kaabar Tal on 3 Mar. 2020 based on Sentinel-2 (**a**), true colour composites (**b1** and **c1**) and corresponding WCTs (**b2** and **c2**) using a handheld VNIR camera. The wetland is rich in submergent and emergent aquatic vegetations (**d**) which got classified as V and WV WCTs in both satellite as well as in-situ imageries (**a2** and **c2**)

freshwater inputs from terrestrial systems, making the water highly turbid and visible in open water regions (Fig. 8(d1)). However, while the high-resolution handheld camera captured this turbid WCT (Fig. 8(d2)), Sentinel-2, due to moderate spatial resolution, could not sense it and classified these regions as WV type.
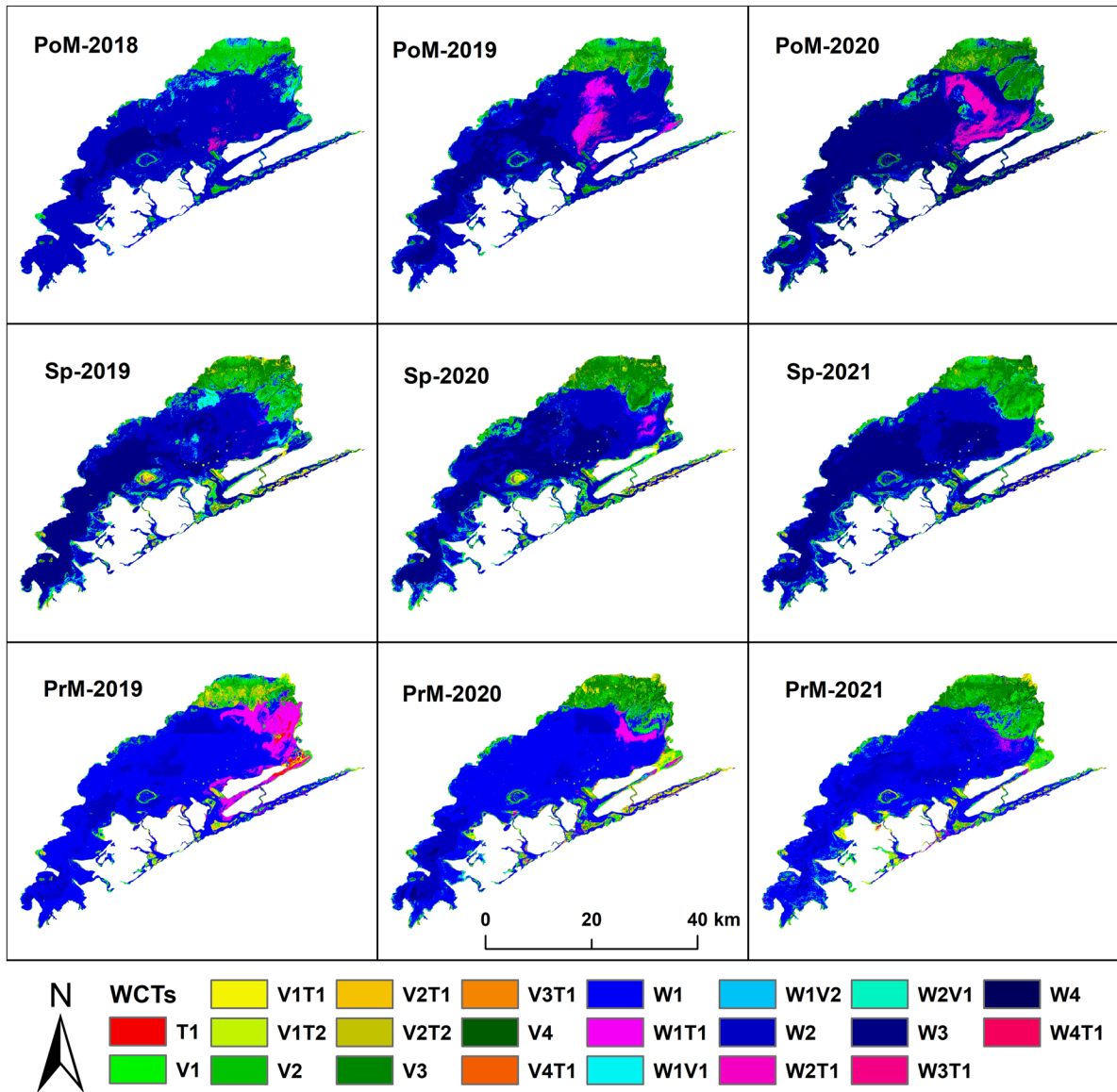
Fig. 6 Seasonal WCTs of Chilika Lake for period 2018–2021. PoM: post-monsoon; Sp: spring; PrM: pre-monsoon

Nal Sarovar

Located in a semi-arid region, the Nal Sarovar displays rapid seasonal changes in wetland cover types (Fig. 9). A rainfall deficit year 2018 (India-WRIS, 2022) resulted in very drastic change in WCTs for this wetland when it remained completely dry in all three seasons except for a very small open water patch (1.9 km^2) in the post-monsoon. For the other 2 years, i.e., 2019–2020 and 2020–2021, the rainfall was surplus, resulting in large open water areas in the wetland in post-monsoon and spring seasons and a relatively wetter condition in pre-monsoon. In the post-monsoon, open water WCTs can be observed in the northern and southern parts of the wetland. However, such WCTs are limited to the northern parts only in the spring. In pre-monsoon, most parts of the wetland remain dry and transform into VT type, with some W and V types in the north-central regions.

The seasonal transformation of WCTs for a recent period (2020–2021) is illustrated in Fig. 10. In the
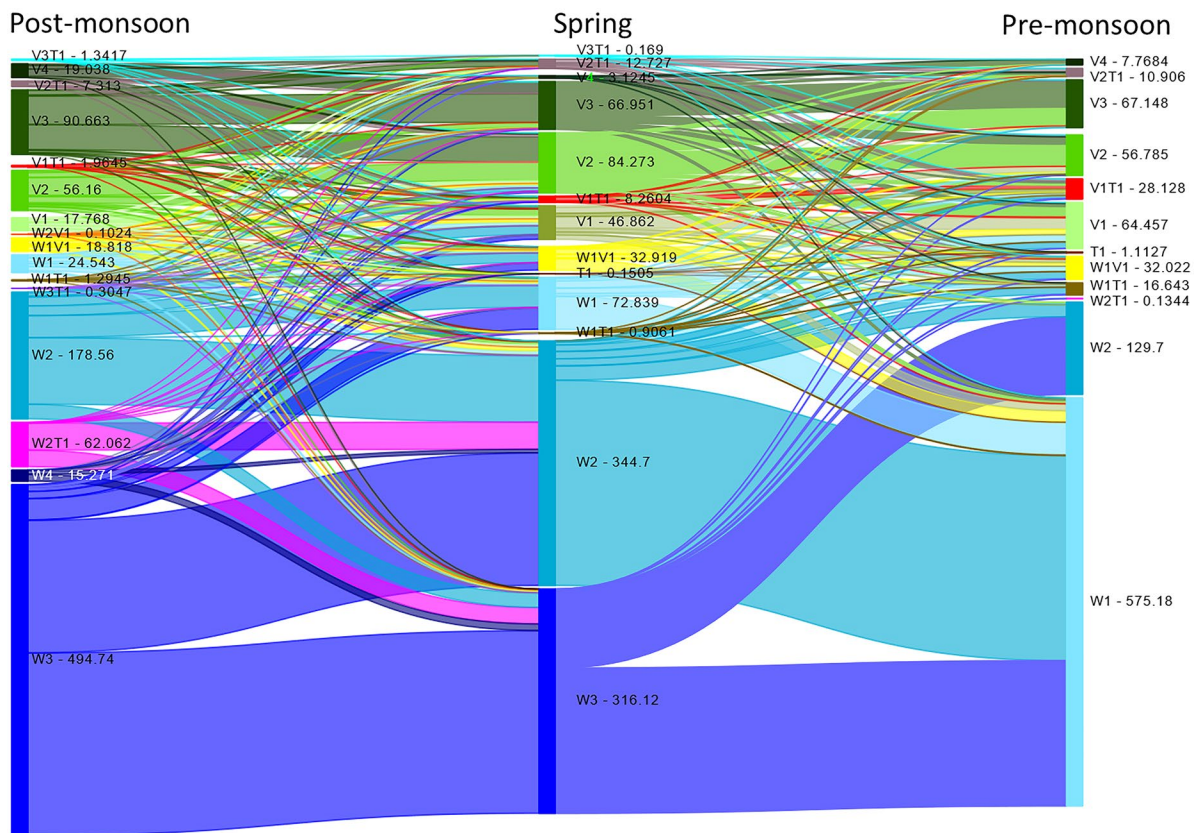
Fig. 7 Seasonal transformation of WCTs in Chilika Lake in year 2020–2021. Numbers are representing areas of corresponding WCT in km^2

post-monsoon period of 2020, about two-thirds of the wetland was covered by V-type WCT, and only about 5.5% of wetland had open water. In the spring of 2021, most of the V types were transformed into VT, and this WCT covered 55% of the wetland area. Most parts of the wetland with low water cover (W1) in the post-monsoon period are transformed into other WCTs in spring; however, medium water cover (W2) remained unchanged between these two seasons. Further, about 81% of the wetland is covered by VT type in pre-monsoon season, and the open water (W) class covers only 1 km^2 of the wetland area in sharp contrast to ~ 14 km^2 in spring. Some parts of the wetland with V1 type show an interesting transformation between wetter and drier seasons—they are getting converted into higher vegetation classes V2 and V3. This implies that with increasing drying, the vegetation cover of these parts is getting denser. Water cover with turbidity (WT)

is negligible in all three seasons. Aquatic vegetation (WV) cover reduces to half in spring with respect to post-monsoon and then to less than one-third of spring in pre-monsoon. Most parts covered with W1V1 class during post-monsoon are converted to V1 in spring, and then to V2 in pre-monsoon.

Discussion

Applicability of WCTs to understand wetland complexities

Wetlands are heterogeneous landscapes with various biotic and abiotic components in the water body and on the water surface, making mapping WCTs a complicated task (Dronova et al., 2011; Mozumder et al., 2014; Wright & Gallant, 2007). The surface covers can be composed of a mixture of classes in
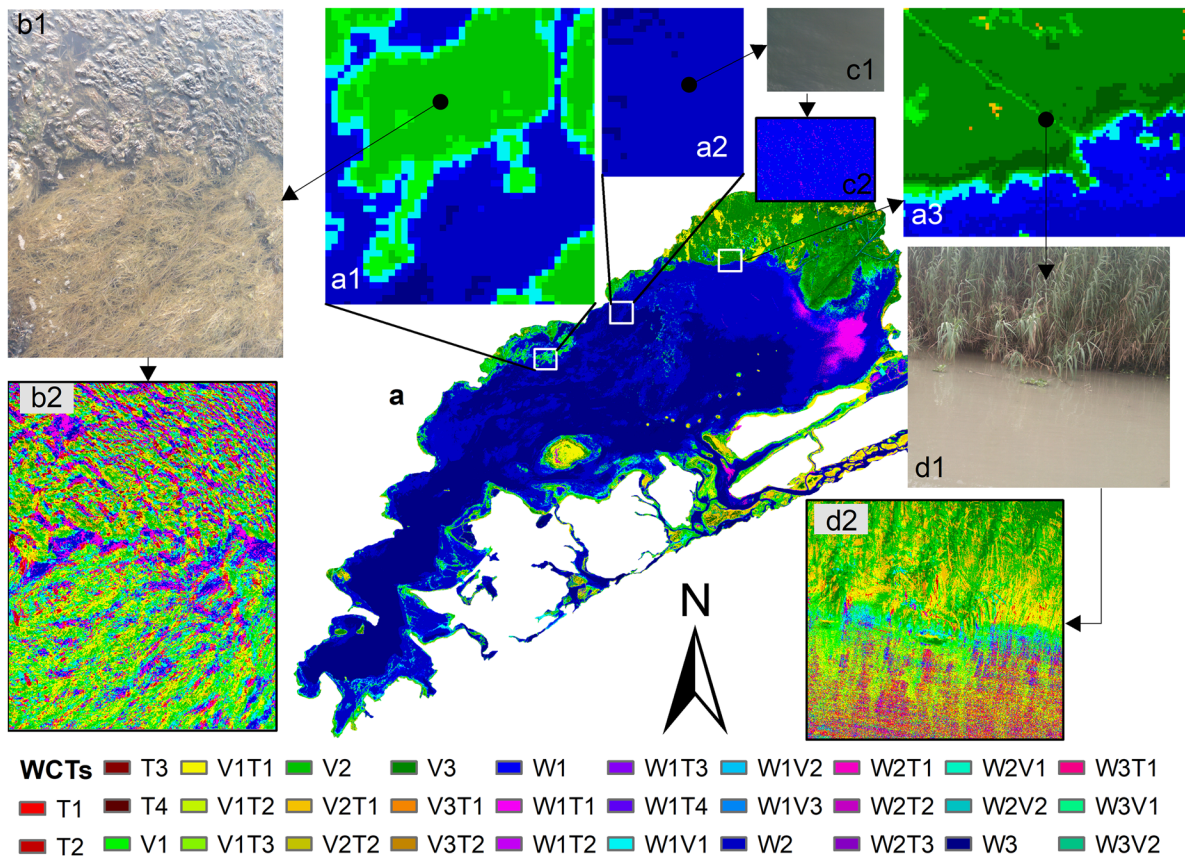
Fig. 8 Field validation—WCT classes of Chilika Lagoon (3 Mar. 2020) based on Sentinel-2 (**a**), true colour composites (**b1**, **c1**, and **d1**) and corresponding WCTs (**b2**, **c2**, and **d2**) using a handheld VNIR camera. See text for explanation of images in inset

space and may have various transitional states in time (Dronova et al., 2015). Therefore, the dynamic nature of wetlands warrants evaluation techniques that can account for rapidly transforming landscapes within a wetland. Methods such as ISO-clustering using multispectral indices and Forel-Ule colour scale can generate distinct patches of wetland covers as illustrated for Chilika (Fig. 11). However, the unsupervised classification techniques such as ISO-clustering result in random classes (Fig. 11b), and the underlying biophysical processes responsible for such classes cannot be ascertained without extensive in-situ measurements. The Forel-Ule colour scale method works only with open water systems and fails with other cover types. For example, the northern parts of the Chilika, otherwise covered with vegetation, are classified as open water on the Forel-Ule scale (Fig. 11c). The proposed WCT scheme can not only identify distinct classes

as in ISO-clustering and Forel-Ule colour scheme, including the non-water cover types, but it also provides crucial information about the underlying biophysical processes (Fig. 11d).

Several workers have used the WCT approach before for wetland monitoring and management but in a rather limited context. For example, Hu et al. (2021) and Zhang et al. (2021) have recently used the WCT approach to evaluate wetland dynamics. However, the WCTs defined by Hu et al. (2021) mainly represent the geomorphic characterisation of wetlands and not the wetland cover types. Similarly, the classes defined by Zhang et al. (2021) are a combination of wetland cover and geomorphic settings. Further, a common limitation of most of the previous studies on WCT (e.g., Dronova et al., 2011, 2015; Fang et al., 2016; Mozumder et al., 2014; Trama et al., 2009) is that the WCT classes are static, and there is no mechanism to include the transitional classes. Although Mozumder
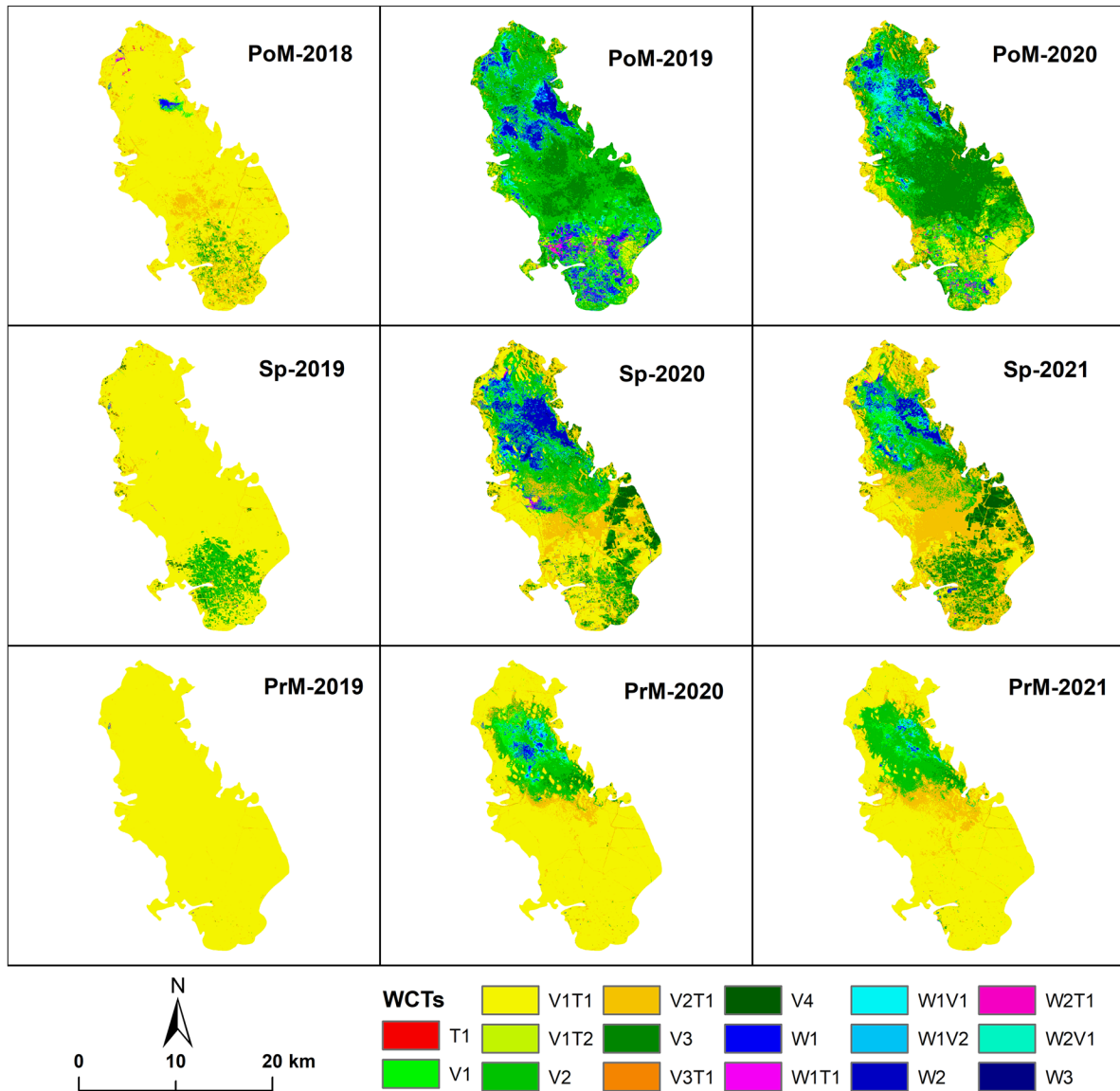
Fig. 9 Seasonal WCTs of Nal Sarovar for period 2018–2021. PoM: post-monsoon; Sp: spring; PrM: pre-monsoon

et al. (2014) had a transitional class, it included a mixture of different classes, and therefore, did not provide any information about the biophysical processes responsible for specific transitions. The WCT approach of Dronova et al. (2015) deals with dynamic transition of classes by defining different transition pathways over a time period. However, this approach also does not account for new transitional classes, and since the classes are defined over a period, it is challenging to evaluate seasonal dynamics.

Further, most of these schemes are designed for a single wetland and therefore they are site-specific. For example, Fang et al. (2016) and Mozumder et al. (2014) used decision tree classification with site-specific thresholds to define WCT classes. Therefore, it is difficult to apply these approaches to a regional/basin scale encompassing numerous wetlands. In the proposed approach in this paper, transitional classes are accounted for by keeping the WCT classes dynamic. For example, if the vegetation cover over a wetland increases from low to very
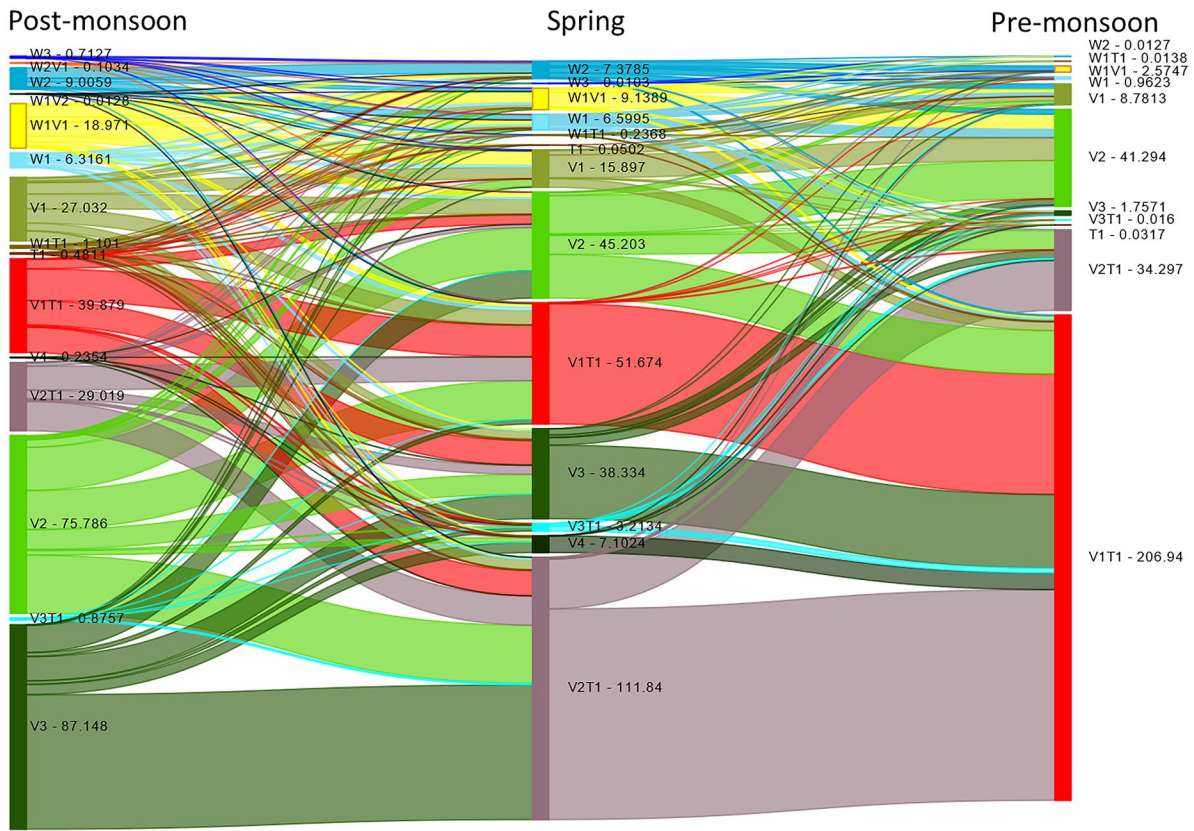
Fig. 10 Seasonal transformation of WCTs in Nal Sarovar in year 2020–2021. Numbers are representing areas of corresponding WCT in km^2

high, a new class V4 will automatically replace V1 without changing the algorithm. Further, since the classes are defined using equal intervals of WCT indices without calibrating them to a particular wetland, the algorithm can be applied to any wetland. A wide applicability of the proposed algorithm has been demonstrated in this paper for three very different wetland systems of India. If needed, this algorithm can be calibrated to a given wetland by changing suitable thresholds to the WCT indices. Therefore, the proposed algorithm can be used as a generalised approach for mapping WCT for a specific wetland, and therefore, it will serve as a powerful tool for monitoring wetland health.

Inter-sensor comparison of WCTs

The proposed WCT classification is designed to be independent of the imaging sensor, i.e., the method can be applied with any sensor providing images in VNIR

bands—green, red, and NIR. However, wetlands possess a steep environmental gradient, resulting in short ecotones (Zomer et al., 2009). This implies that ecological and hydrological characters might change rapidly within a few metres, rendering the WCT classification method dependent on the spatial resolution of the imaging sensor (e.g., field validation Figs. 5 and 8). Therefore, to understand the effect of spatial resolution of the sensors, we have applied the method on two widely used and freely available multispectral satellite datasets—Landsat-8 (30 m spatial resolution) and Sentinel-2 (10 m spatial resolution for VNIR bands). We observed that for large WCT patches, results from both the sensors are similar (Fig. 12). However, in the regions of high variability, Sentinel-2 identifies a larger number of WCTs compared to those from Landsat-8. Similar results were reported by Sánchez-Espinosa and Schröder (2019) when they compared the suitability of Landsat-8 and Sentinel-2 for LULC classification
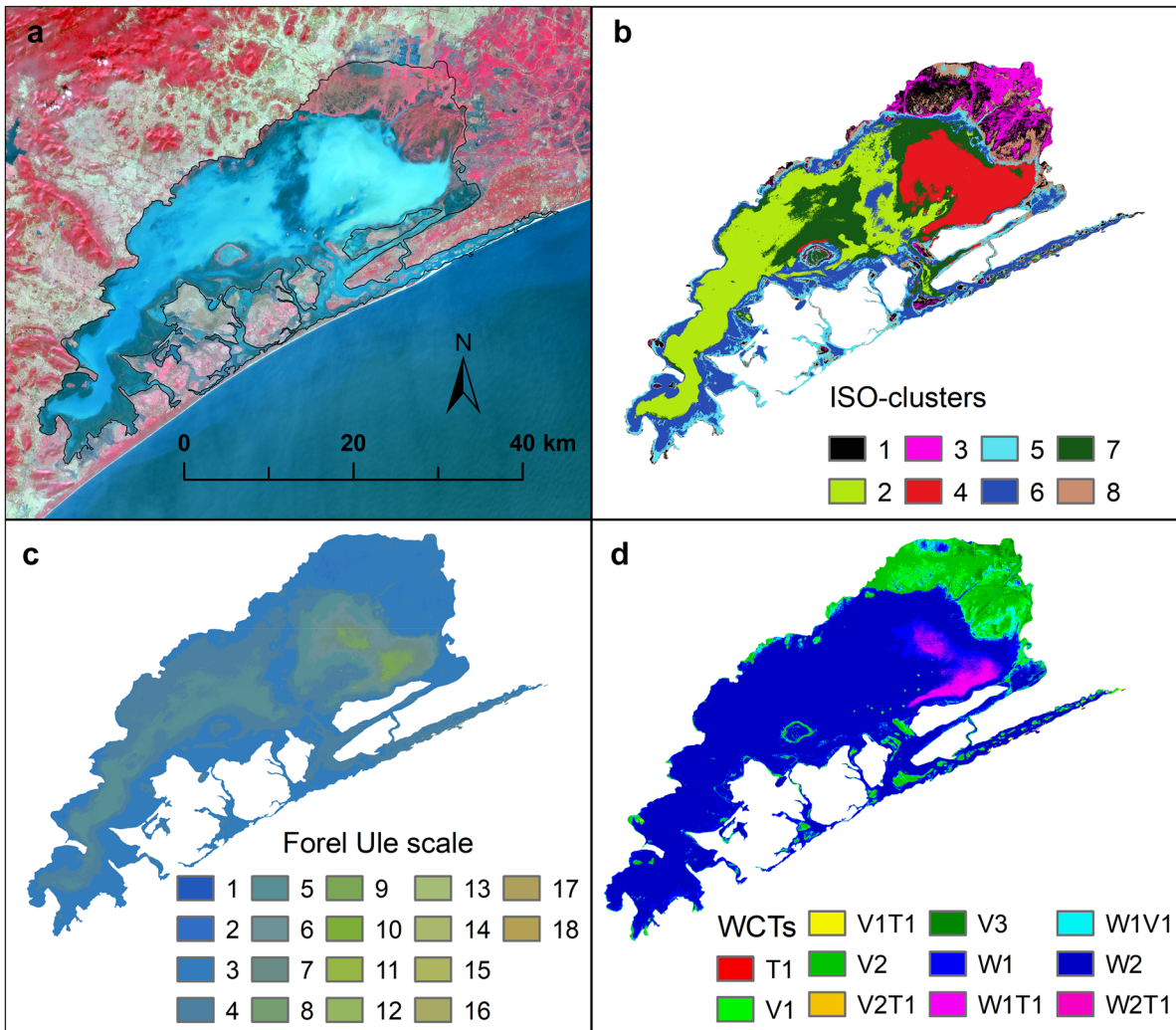
Fig. 11 Comparison of various methods for waterbody surface dynamics assessment. **a** A standard FCC of Chilika Lake. **b** ISO-clustering of three WCT indices—NDWI, NDVI, and NDTI. **c** Forel-Ule colour scales. **d** WCTs. All are based on same Sentinel-2 data dated 1 Feb. 2021

in a wetland environment. Their study showed that Sentinel-2 performed better than Landsat-8 in complex areas. However, both sensors performed similarly for areas with large patches of similar LULC type. This was attributed to the fact that a single pixel in a medium-resolution Landsat image (30 m) might consist of a mixture of various wetland covers, but only the dominant type gets captured by the sensor. We observed a similar behaviour when we compared the WCTs obtained by a handheld multispectral camera in the field with those based on Sentinel-2 imagery (Figs. 5 and 8). When there are large WCT patches,

pixels are pure and not mixed, and there is no serious impact of spatial resolution, as seen in Fig. 12. Mixed pixels occur because of the low resolution of the imaging sensor where multiple ground objects are combined in a single pixel or when the ground object is a homogenous mixture of various materials (Keshava, 2003; Shimabukuro & Smith, 1991). Therefore, the spectra of a single pixel contain a record of various materials (Quintano et al., 2012). Furthermore, although the radiometric characteristics of Sentinal-2 and Landsat-8 are similar, they are not identical (Mandanici & Bitelli, 2016). Also, they have different heights and azimuth.
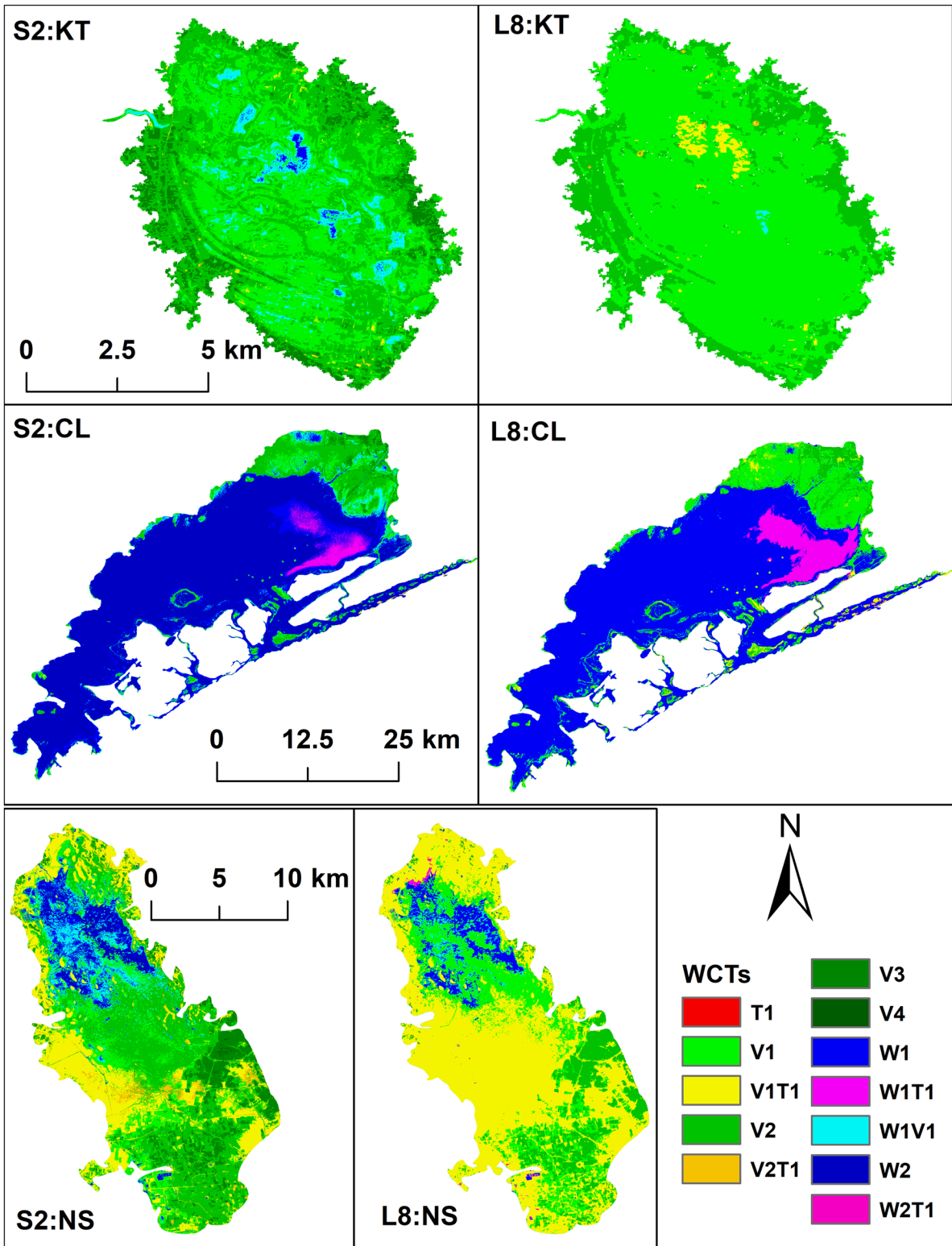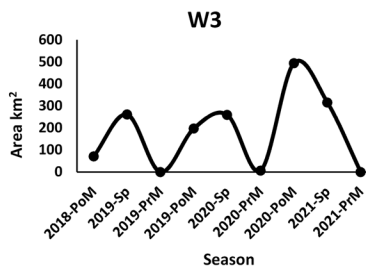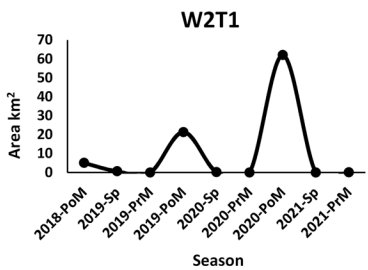
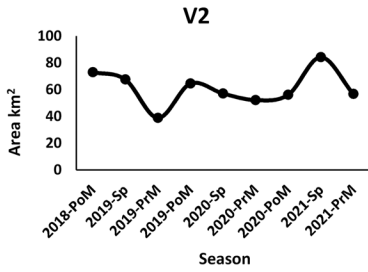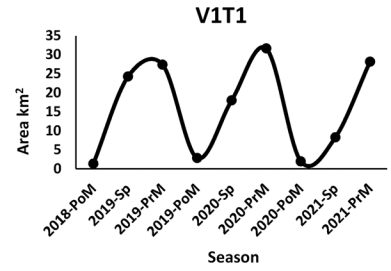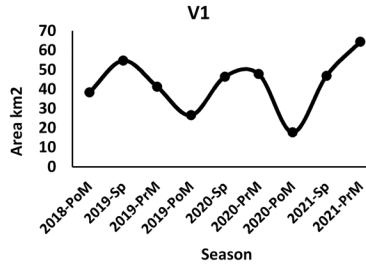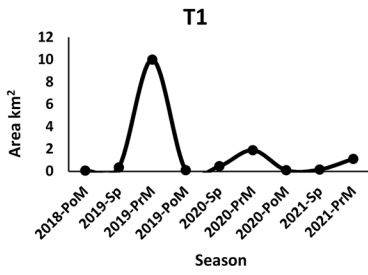**Fig. 12** Inter-sensor (S2: Sentinel-2, L8: Landsat-8) comparison for all three wetlands KT (Kaabar Tal), CL (Chilika Lake), and NS (Nal Sarovar)
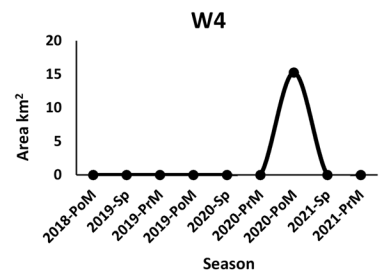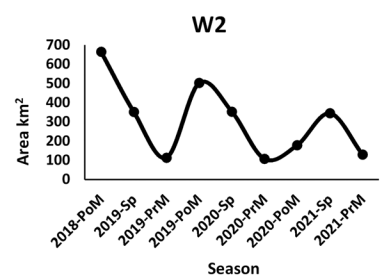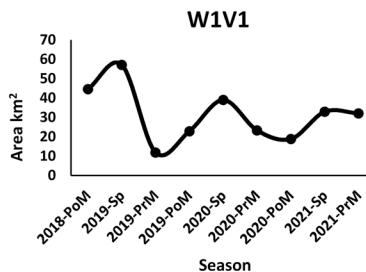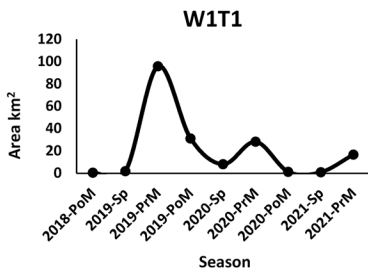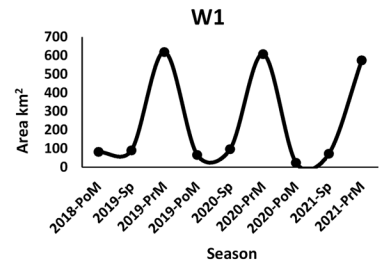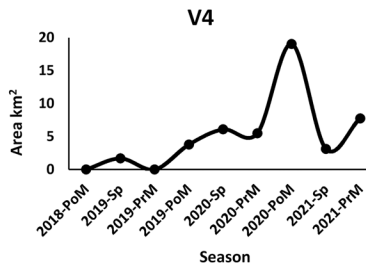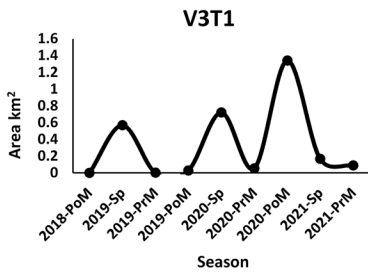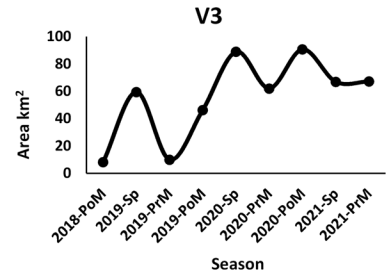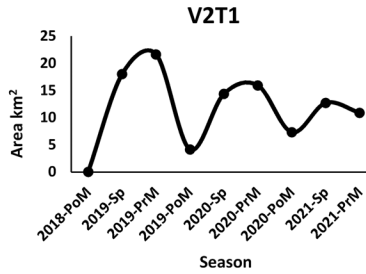
◄**Fig. 13** A WCT-wise trend assessment for Chilika Lake. Seasonal cyclicities are evident in most of the WCTs. A deviation from a predicted behaviour can be an indicator of a change in underlying biophysical properties of a wetland

Therefore, identical results from Sentinel-2 and Landsat-8 should not be expected, and in any time series WCT study, only one sensor should be used.

Utility of WCT for wetland management and long-term monitoring

Wetlands are complex and dynamic ecosystems and possess various abiotic and biotic connectivity with other landscape elements (Cohen et al., 2016; Thorslund et al., 2017). They are well known for their species richness, and their anthropogenic degradation makes them a conservation priority in most landscapes (Catallo, 1993). Usually, wetland restoration efforts aim to improve the quality of habitats, support species' resilience to climate and land cover changes, and restore ecological and hydrological services (Taddeo & Dronova, 2018). Identification of a suitable spatio-temporal scale for wetland monitoring is necessary for planning and executing the management strategies (Steinbach et al., 2021). This can be achieved by creating long-term datasets. The multi-decadal Landsat series satellite imageries can be used to generate such long-term datasets. Long-term and continuous monitoring can help wetland managers to plan the restoration efforts and evaluate their impact. In this context, it is essential to (a) track the usual WCTs of a wetland and their spatio-temporal trend, and (b) look for new WCTs as and when they develop to understand their significance in terms of wetland health. The proposed WCT approach can be used to realise such wetland monitoring goals for a comprehensive wetland management and restoration.

For example, in the case of the Chilika, all possible WCTs are shown in Fig. 13 encompassing 3 years, namely, 2018–2019, 2019–2020, and 2020–2021. We noted some specific trends associated with different WCTs. There are WCTs such as V1T1 and W1 that follow the same trend in all years. The WCTs V3 and V2T1 have changed their patterns in recent years, and T1 and W4 are only present in a few seasons and years. Therefore, with an extended assessment period,

the characteristic WCTs of a given wetland can be identified and used as benchmarks for the health of that wetland. The sudden appearance of new WCTs and abrupt changes in the trends of characteristic WCTs can prove to be useful indicators of wetland health and can also guide the restoration approach.

In case of Kaabar Tal, it was observed that the water-related cover types of the wetland, i.e., Ws are mostly negligible in all three seasons (Figs. 3 and 4). Whenever present, they are readily transformed into another WCT in the next season. It implies that this wetland is hydrologically highly distressed—a crucial conclusion from the time-series WCT assessment. A previous study on Kaabar noted a statistically significant decreasing trend of wetness and a statistically significant increasing trend of vegetation cover in this wetland, and this was attributed to intensified agricultural activities (Singh & Sinha, 2021a). To assess the tipping point when such wetlands are transformed from wetness dominated system to vegetation dominated system, the time-series WCT assessment using archival Landsat satellite series can be extremely useful. Such analysis could have a significant impact on designing management and restoration strategies of this highly water-stressed wetland which has been recently designated as a Ramsar site.

Further, the WCT assessment of Nal Sarovar shows high vegetation growth in its central region after the monsoon season (September–October), which could be an algal bloom. During the same season, the extent of the open water area is the highest in the whole year. Therefore, the monsoon-controlled runoff into the wetland is responsible for the spatial distribution of WCTs. The increment in vegetation area and vegetation-related WCT implies that the runoff reaching the wetland after monsoon rainfall is nutrient-loaded which encourages the growth of biomass. This might increase the wetland's BOD (biological oxygen demand), and therefore, stressing its ecosystem. Further, it is a turbidity-dominated wetland, possibly because of the small aquaculture in its vicinity. Turbidity-related WCTs are observed for an extended period from January to June. Therefore, similar to the other two wetlands, the monthly WCTs can help in understanding the wetland's seasonal biotic and abiotic dynamics, and to design relevant season-specific management practices.

Conclusions

We have developed a multispectral imagery-based monitoring and change detection method for mapping and monitoring wetland covers. The algorithm to map the WCT classes is implemented in the GEE environment and can be applied to any wetland. We have also developed GIS tools to automatically calculate WCTs for any sensor-producing imagery in VNIR bands. The specific conclusions drawn from this work are as follows:

1. Unlike the popular methods such as ISO-clustering and Forel-Ule Colour schemes which either generate random classes or work for open water systems only, our approach can be applied to a wide variety of settings and can provide crucial information about the underlying biophysical processes.
2. The developed algorithm generates the WCT classes that are stable in time and space. This means that the same WCT class represents the similar underlying biophysical property of the wetland across space and time, making it appropriate for wetland monitoring and change detection. Nevertheless, the number of the WCT classes is dynamic and can account for any new cover type emerging in a wetland by automatically adding a new WCT class.
3. Our results clearly demonstrate the control of local hydrogeomorphic conditions on the spatial and temporal distribution of WCTs, and therefore, highlights the complexities of wetland environments. For example, the lack of water-related WCTs at Kaabar is indicative of its hydrologically stressed condition whereas the frequent inter-transformation of water and vegetation-related WCTS at Chilika indicates a very dynamic system. The Nal Sarovar displays a significant increment in vegetation-related WCT in different seasons suggesting the influx of nutrient-loaded runoff.
4. An important finding is that whilst our proposed WCTs are independent of the imaging sensor as long as they provide data in VNIR bands. However, the spatial resolution of different sensors can create some differences primarily because of mixed pixels. It is therefore recommended to use data from one sensor only for time series analysis for reliable results.

It is important to note that the proposed algorithm uses three commonly used multispectral indices (NDVI, NDWI, NDTI), and therefore, all limitations associated with these indices are also associated with the generated WCTs, such as misidentification of dry soils as turbid class and ambiguity between aquatic vegetation and terrestrial vegetation. However, such issues can be rectified by using supporting information from field validation and the SAR datasets as and when required. For example, SAR datasets such as the proposed NISAR (NASA-ISRO SAR) mission (dual-frequency S and L bands) can be used to pre-classify wet and dry regions since its L-band can penetrate vegetation cover.

In its current form, the algorithm is best suited for the rapid assessment and monitoring of a large number of wetlands, including several Ramsar sites, for country-scale wetland health assessment projects. It is hoped that several case studies on wetlands from different hydrogeomorphic settings across the globe would benefit from this approach. Further refinement of this approach should be possible using high-resolution hyperspectral data from airborne missions that could provide specific information about water quality parameters which could be integrated with wetland cover types.

Declarations

Conflict of interest The authors declare no competing interests.

References

Ambastha, K., Hussain, S. A., & Badola, R. (2007). Resource dependence and attitudes of local people toward conservation of Kabartal wetland: A case study from the Indo-Gangetic plains. *Wetlands Ecology and Management, 15*(4), 287.

Catallo, W. J. (1993). Ecotoxicology and wetland ecosystems: Current understanding and future needs. *Environmental Toxicology and Chemistry: An International Journal, 12*(12), 2209–2224.

Chauhan, M. (2003). Conserving biodiversity in arid regions: Experiences with protected areas in India. In: L. J., V. R. & S. D. (Eds.), Conserving Biodiversity in Arid Regions. Springer, Boston, MA, pp 231–248.

Cohen, M. J., Creed, I. F., Alexander, L., Basu, N. B., Calhoun, A. J., Craft, C., D'Amico, E., DeKeyser, E., Fowler, L., & Golden, H. E. (2016). Do geographically isolated wetlands influence landscape functions? *Proceedings of the National Academy of Sciences, 113*(8), 1978–1986.

Davidson, T. A., Mackay, A. W., Wolski, P., Mazebedi, R., Murray-Hudson, M., & Todd, M. (2012). Seasonal and spatial hydrological variability drives aquatic biodiversity in a flood-pulsed, sub-tropical wetland. *Freshwater Biology, 57*(6), 1253–1265.

Dottavio, C. L., & Dottavio, F. D. (1984). Potential benefits of new satellite sensors to wetland mapping. *Photogrammetric Engineering & Remote Sensing, 50*(5), 599–606.

Dronova, I., Gong, P., & Wang, L. (2011). Object-based analysis and change detection of major wetland cover types and their classification uncertainty during the low water period at Poyang Lake. *China. Remote Sensing of Environment, 115*(12), 3220–3236.

Dronova, I., Gong, P., Wang, L., & Zhong, L. (2015). Mapping dynamic cover types in a large seasonally flooded wetland using extended principal component analysis and object-based classification. *Remote Sensing of Environment, 158*, 193–206.

Ernst-Dottavio, C. L., Hoffer, R. M., & Mroczynski, R. P. (1981). Spectral characteristics of wetland habitats. *Photogrammetric Engineering & Remote Sensing, 47*(2), 223–227.

Fang, C., Tao, Z., Gao, D., & Wu, H. (2016). Wetland mapping and wetland temporal dynamic analysis in the Nanjishan wetland using Gaofen One data. *Annals of GIS, 22*(4), 259–271.

Finlayson, C.M., Rastogi, G., Mishra, D.R. & Pattnaik, A.K. (2020) Ecology, conservation, and restoration of Chilika Lagoon, India, 6.

Forel, F. A. (1890). Une nouvelle forme de la gamme de couleur pour l'étude de l'eau des lacs. *Archives des sciences physiques et naturelles/Societe de physique et d'histoire naturelle de geneve, 6*(25).

Gehrels, J., & Mulamoottil, G. (1990). Hydrologic processes in a southern Ontario wetland. *Hydrobiologia, 208*(3), 221–234.

Hess, T.M., Morris, J., Gowing, D.G., Leeds-Harrison, P.B., Bannister, N., Vivash, R.M. & Wade, M. (2003). Integrated washland management for flood defence and biodiversity, international conference towards natural flood reduction strategies, Warsaw, pp 6–13.

Hu, X., Zhang, P., Zhang, Q., & Wang, J. (2021). Improving wetland cover classification using artificial neural networks with ensemble techniques. *Giscience & Remote Sensing, 58*(4), 603–623.

India-WRIS. (2022). RainFall report - DISTRICTWISE - (SUM) (ALL AGENCIES) : 2011 - 2021. India Water Resources Information System, Online.

Jiménez-Rodríguez, C. D., Esquivel-Vargas, C., Coenders-Gerrits, M., & Sasa-Marín, M. (2019). Quantification of the evaporation rates from six types of wetland cover in Palo Verde National Park. *Costa Rica. Water, 11*(4), 674.

Joshi, K., Tatu, K., & Kamboj, R. (2020). Seasonal assessment of aquatic avifauna of Nal Sarovar Sanctuary, Gujarat. *India. Indian Forester, 146*(10), 917–923.

Keshava, N. (2003). A survey of spectral unmixing algorithms. *Lincoln Laboratory Journal, 14*(1), 55–78.

Mandanici, E., & Bitelli, G. (2016). Preliminary comparison of sentinel-2 and landsat 8 imagery for a combined use. *Remote Sensing, 8*(12), 1014.

Moore, T. S., Dowell, M. D., Bradt, S. & Ruiz Verdu, A. (2014). An optical water type framework for selecting and blending retrievals from bio-optical algorithms in lakes and coastal waters. *Remote Sensing of Environment, 143*(Supplement C), 97–111.

Mozumder, C., Tripathi, N., & Tipdecho, T. (2014). Ecosystem evaluation (1989–2012) of Ramsar wetland Deepor Beel using satellite-derived indices. *Environmental Monitoring and Assessment, 186*(11), 7909–7927.

Murthy, T., & Panigrahy, S. (2011). Monitoring of structural components and water balance as an aid to wetland management using geospatial techniques–A case study for Nalsarovar Lake, Gujarat. *International Archives of the Photogrammetry, Remote Sensing and Spatial Information Sciences, 38*(8/W20).

Oestreich, W. K., Chapman, M. S., & Crowder, L. B. (2020). A comparative analysis of dynamic management in marine and terrestrial systems. *Frontiers in Ecology and the Environment, 18*(9), 496–504.

Quintano, C., Fernández-Manso, A., Shimabukuro, Y. E., & Pereira, G. (2012). Spectral unmixing. *International Journal of Remote Sensing, 33*(17), 5307–5340.

RIS, R.I.S. (2012). Information Sheet on Ramsar Wetlands (RIS): Ramsar Site no. 2078

Sánchez-Espinosa, A., & Schröder, C. (2019). Land use and land cover mapping in wetlands one step closer to the ground: Sentinel-2 versus landsat 8. *Journal of Environmental Management, 247*, 484–498.

Shimabukuro, Y. E., & Smith, J. A. (1991). The least-squares mixing models to generate fraction images derived from remote sensing multispectral data. *IEEE Transactions on Geoscience and Remote Sensing, 29*(1), 16–20.

Singh, M., & Sinha, R. (2020). Distribution, diversity, and geomorphic evolution of floodplain wetlands and wetland complexes in the Ganga plains of north Bihar. *India. Geomorphology, 351*, 106960.

Singh, M., & Sinha, R. (2021a). Hydrogeomorphic indicators of wetland health inferred from multi-temporal remote sensing data for a new Ramsar site (Kaabar Tal). *India. Ecological Indicators, 127*, 107739.

Singh, M., & Sinha, R. (2021b). Kaabar Tal, Bihar's first Ramsar site: Status, challenges and recommendations. *Current Science, 120*(2), 270–272.

Singh, M., & Sinha, R. (2022). A basin-scale inventory and hydrodynamics of floodplain wetlands based on time-series of remote sensing data. *Remote Sensing Letters, 13*(1), 1–13.

Singh, M., Sinha, R., Mishra, A. & Babu, S. (2022). Wetlandscape (dis)connectivity and fragmentation in a large wetland (Haiderpur) in west Ganga plains, India. *Earth Surface Processes and Landforms, 1–16.

Sinha, R., Gupta, S., & Nepal, S. (2018). Groundwater dynamics in North Bihar plains. *Current Science, 114*(12), 2482–2493.

Sinha, R., Saxena, S., & Singh, M. (2017). Protocols for riverine wetland mapping and classification using remote sensing and GIS. *Current Science, 112*(7), 1544–1552.

Steinbach, S., Cornish, N., Franke, J., Hentze, K., Strauch, A., Thonfeld, F., Zwart, S. J., & Nelson, A. (2021). A new conceptual framework for integrating Earth observation in large-scale wetland management in East Africa. *Wetlands, 41*(7), 93.

Taddeo, S., & Dronova, I. (2018). Indicators of vegetation development in restored wetlands. *Ecological Indicators, 94*, 454–467.

Tatu, K., Parihar, J. S., & Kimothi, M. (1999). *Remote sensing for wetland monitoring & waterfowl habitat management: A case study of Nal Sarovar (Gujarat)* (p. 177). APH Publishing.

Thorslund, J., Jarsjo, J., Jaramillo, F., Jawitz, J. W., Manzoni, S., Basu, N. B., Chalov, S. R., Cohen, M. J., Creed, I. F., & Goldenberg, R. (2017). Wetlands as large-scale nature-based solutions: Status and challenges for research, engineering and management. *Ecological Engineering, 108*, 489–497.

Todd, A. K., Buttle, J. M., & Taylor, C. H. (2006). Hydrologic dynamics and linkages in a wetland-dominated basin. *Journal of Hydrology, 319*(1–4), 15–35.

Trama, F. A., Rizo-Patrón, F. L., Kumar, A., González, E., & Somma, D. (2009). Wetland cover types and plant community changes in response to cattail-control activities in the Palo Verde Marsh. *Costa Rica. Ecological Restoration, 27*(3), 278–289.

Ule, W. (1892). Die bestimmung der Wasserfarbe in den Seen. Kleinere Mittheilungen. Dr. A. Petermanns Mittheilungen aus Justus Perthes geographischer Anstalt, 70–71.

Wright, C., & Gallant, A. (2007). Improved wetland remote sensing in Yellowstone National Park using classification trees to combine TM imagery and ancillary environmental data. *Remote Sensing of Environment, 107*(4), 582–605.

Ye, M., & Sun, Y. (2022). Review of the Forel–Ule index based on in situ and remote sensing methods and application in water quality assessment. *Environmental Science and Pollution Research,* 1–18.

Zhang, X., Fu, S., Hu, Z., Zhou, J., & Zhang, X. (2021). Changes detection and object-oriented classification of major wetland cover types in response to driving forces in Zoige County, Eastern Qinghai-Tibetan Plateau. *IEEE Journal of Selected Topics in Applied Earth Observations and Remote Sensing, 14*, 9297–9305.

Zomer, R. J., Trabucco, A., & Ustin, S. L. (2009). Building spectral libraries for wetlands land cover classification and hyperspectral remote sensing. *Journal of Environmental Management, 90*(7), 2170–2177.